

ŁUKASZ KARWOWSKI & ROMAN WŁODYKA

## Stannite in the cassiterite-sulfide deposits of the Iżera Mts (Sudetes)

**ABSTRACT:** Stannite, found by mineralogical studies in the cassiterite-sulfide deposits of the Kamiénica Chain (Iżera Mts), being almost perfectly of theoretical composition, occurs in paragenesis with chalcopyrite, sphalerite, pyrrhotite and other diverse sulphides. Newly recognized post-sulfide cassiterite was probably formed by stannite decomposition. The presence of stannite proves hydrothermal origin of the cassiterite-sulfide mineralization of the Iżera Mts.

### INTRODUCTION

Cassiterite-sulfide mineralization in the northern slopes of the Iżera Mts in the western Sudetes (Text-fig. 1; cf. also Kowalski, Karwowski & al. 1978) occurs in either two or three levels intercalating mica-chlorite schists of the Kamiénica Chain. Ore-bearing zones vary in thickness and in mineral composition.

Previous works (Sachs 1914, Stehr 1933, Putzer 1940, Jaskólski & Mochnacka 1958, Sałaciński 1965, Kowalski, Karwowski & al. 1978) revealed in the local hydrothermal association several ore assemblages, beginning with cassiterite-thuringite-quartz and overlapped in the final stage with polymetal mineralization.

Sulfide sequence depended on the stage of mineralization and local chemical composition of mineralizing solutions. Following ore minerals were recognized: ilmenite, rutile, magnetite, cassiterite, cobaltite, loellingite, arsenopyrite, pyrrhotite, sphalerite, chalcopyrite, cubanite, native bismuth, bismuthinite, bismuth sulfosalts, nickeline, tetrahedrite, boulangierite, bournonite, antimonite, mackinawite, covellite, chalcocite, bornite, melnikovite, marcasite and pyrite.

Origin of the discussed cassiterite ores is still controversial. Most authors support the hydrothermal genesis connected either with the Iżera granite-gneisses (Sachs 1914, Stehr 1933) or with Variscan grani-

toid massif of the Karkonosze Mts (Jaskólski & Mochacka 1958, Birecki 1959, Chilińska 1965, Sałaciński 1965, Kozłowski & Karwowski 1975, Kowalski, Karwowski & *al.* 1978). Competitive opinion on metasedimentary placer formation of the cassiterite mineralization overlapped with significantly later sulfides has been also elaborated (Jaskólski 1963, 1967; Szałamacha 1967, 1970, 1979; Szałamacha & Szałamacha 1974).

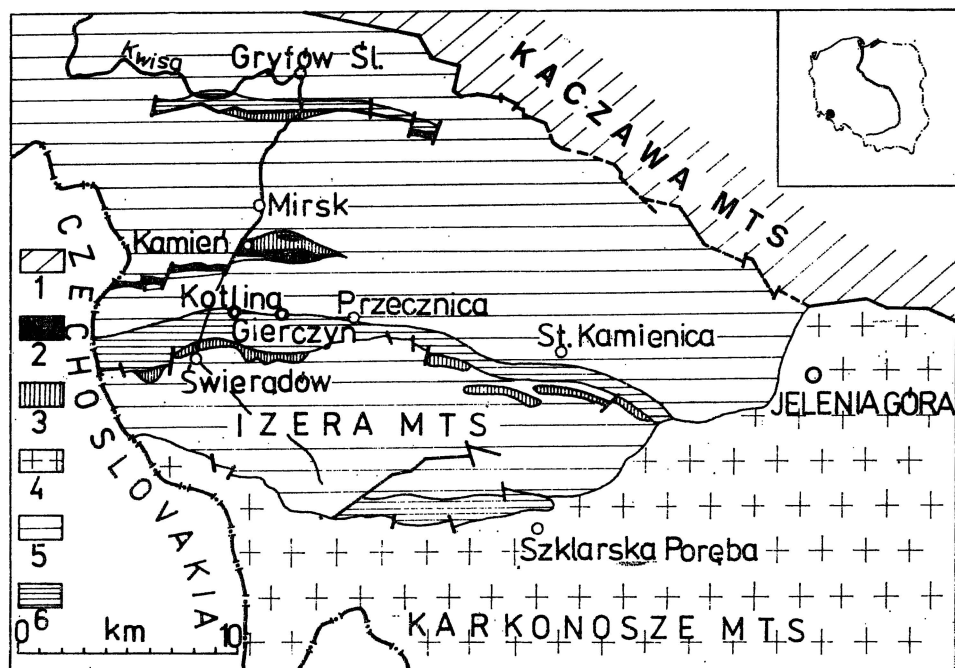


Fig. 1. Schematic sketch map of the Iżera Mts, Western Sudetes (inset shows position of the area in Poland)

1 Metamorphic Kaczawa series, 2 greisens of the Iżera Highland, 3 leucogranites (metasomatic albitites), 4 Karkonosze granitoid, 5 Iżera granite-gneiss, 6 mica and mica-chlorite schists

Stannite in the Sudetes was known hitherto as unique mineralogical findings in the arsenopyrite deposit Czarnów in the Rudawy Janowickie Mts (Schneiderhöhn & Ramdohr 1931, Ramdohr 1975) and paragenetically connected with sphalerite in the polymetallic deposit Słara Góra in the Kaczawa Mts (Zimnoch 1965). Both deposits are connected with the Variscan magmatism.

#### INVESTIGATING METHODS

The investigated samples were collected mostly from dumps of the abandoned mines at Gierczyn and Przecznicza (Fig. 1) and from underground pits mined in 1954–1955 (Gierczyn mine). Specimens for ore microscope and electron-microprobe studies were selected by spectrographical determination of aqua-regia-soluble tin in chalcopyrite, pyrrhotite and sphalerite.

Qualitative and quantitative electron microprobe determinations were performed with use of JEOL JXA 50A probe, applying natural standards: chalcopyrite, stannite, cassiterite.

Authors are very indebted to K. Stróż, M. Sc. and B. Brzycka, M. Sc., in the Institute of Physics and Chemistry of Metals in the Silesian University for help and advices during performed electron microprobe studies.

## RESULTS

Selected chalcopyrite, sphalerite and pyrrhotite specimens rich in Sn (sometimes  $>1$  wt. %) submitted to detailed microscope studies, appeared to contain inclusions of mineral determined by use of its optical features as stannite.

The found stannite has relatively low reflectivity, higher than reflectivity of sphalerite but lower than tetrahedrite. Colour is gray with olive-green tint similar to colour typical of tetrahedrite; bireflectivity is distinct in oil immersion but rarely visible in air (Pl. 1, Fig. 4), changing from olive-brown (darker) to gray-greenish (lighter); anisotropy distinct, especially in immersion, internal reflections not observed. Hardness relatively to neighbouring minerals is lower than for sphalerite but higher than for chalcopyrite.

Surface distribution of tin by electron microprobe analysis in several grains (Pl. 2, Figs 3—4; Pl. 3, Figs 1—2) confirmed presence of tin-bearing mineral which does not bear As, Sb, In, Ag, Zn, Pb and V down to the detection limit, but it bears only Cu, Fe and S. Quantitative electron probe analysis yielded ratios of the above elements almost perfectly calculatable (Table 1) for theoretical stannite formula  $\text{Cu}_2\text{FeSnS}_4$ ; low admixture content suggests low crystallization temperature of stannite (cf. Ramdohr 1975).

Table 1  
Chemical composition of the investigated stannite

Element	Theoretical, %	Stannite from Gierczyn, %
Sn	27.61	27.99
Cu	29.56	29.61
Fe	12.99	12.94
S	29.84	28.47
Total	100.00	99.01

Some stannite grains bear minute inclusions of mineral very light in back-scattered electrons — COMPO (Pl. 2, Fig. 3; Pl. 3, Fig. 1), which only sometimes might be identified as cassiterite.

The microscope studies revealed quite abundant presence of stannite in the specimens studied, especially in close paragenesis with chalcopyrite.

pyrrhotite, pyrrhotite and sphalerite (Pls 1—5), and rarer with Co-arsenopyrite, galena and native bismuth.

Rounded or irregularly shaped stannite inclusions in pyrrhotite (Pl. 1, Figs 1—3) seemed that they are the later mineral, crystallizing in cleavage fissures of pyrrhotite. However, stannite grains used to be cut with the fissures occurring in pyrrhotites (Pl. 1, Fig. 3); together with presence of tiny round stannite grains in non-fractured pyrrhotite this proves a simultaneous crystallization of these two minerals.

Sometimes stannite occurs at the edges of pyrrhotite grains (Pl. 2, Fig. 2) or at the pyrrhotite/sphalerite boundaries (Pl. 3, Fig. 3). Most frequently stannite occurs with chalcopyrite and sphalerite (Pl. 2, Figs 1—2; Pl. 3, Fig. 4; Pl. 5, Figs 1—4), what may be explained by homotype features of these minerals. Intergrowths of stannite and sphalerite (Pl. 1, Fig. 4) or stannite with sphalerite and pyrrhotite (Pl. 4, Fig. 1) dispersed in chalcopyrite occur quite commonly.

Elongated parallel grains of sphalerite and stannite were found (Pl. 4, Fig. 2), often at edges of chalcopyrite, what may be explained as exsolution structures of homotype minerals or parallel intergrowths.

Certain stannite inclusions in chalcopyrite are very similar to sphalerite "asterisks" abundant in some chalcopyrites (Pl. 4, Figs 3—4). Also myrmekite-type stannite/galena or stannite/sphalerite intergrowths were observed.

Spatial relations between stannite and cassiterite suggest that grainy cassiterite is earlier than stannite (Pl. 5, Figs 1—3). Relatively rare are stannite inclusions in quartz, without contact with other ore minerals.

The authors conclude that stannite crystallized during the main stage of sulfide mineralization, after As minerals, together with pyrrhotite, sphalerite I, chalcopyrite, native bismuth and galena I in the local mineral sequence (cf. Kowalski, Karwowski & *al.* 1978).

Stannite may be altered by secondary processes forming a colloform mixture of ?hydroxides rich in tin.

Several specimens contained usual grainy cassiterite plus its cryptocrystalline variety surrounding sulfides, mostly chalcopyrite and sphalerite (Pl. 6, Figs 1—2), accompanied in other parts of the specimen by stannite. Cryptocrystalline cassiterite, similar to the "spongy" or radial SnO<sub>2</sub> described previously (Jaskólski & Mochnacka 1958; Kowalski, Karwowski & *al.* 1978) is white or brownish due to the presence of iron hydroxides.

The microscope recognition was confirmed by electron probe determinations (Pl. 6, Figs 3—4). Cryptocrystalline cassiterite is clearly later than the grainy one and it presumably formed by the stannite decomposition.

## CONCLUSIONS

The presence of stannite in the cassiterite-sulfide deposits of the Kamienica Chain proves a significant role of tin in sulfide-ore forming solutions, and the continuity of tin ion presence in those solutions during precipitation both of cassiterite and of sulfides. If one considers the hypotheses of origin of the deposits, as presented above: meta-sedimentary cassiterite plus later hydrothermal (Variscan) sulfide mineralization (Szalamacha 1979) or one cycle hydrothermal genesis of the ore of the cassiterite-silicate formation, sulfide-chlorite subtype, thus should be taken into account the following:

(i) High purity of cassiterite. If cassiterite was accumulated in the placer deposits, coming from the hypothetical pre-Variscan granitoids, it should be rich in *e.g.* Fe, Nb, Ta, Sc, whereas the previously studied cassiterite is poor in those elements (Kowalski, Karwowski & *al.* 1978).

(ii) Close paragenetic ties of cassiterite with quartz and chlorite (thuringite type) like in other similar but undoubtedly hydrothermal deposits, *e.g.* in the Sikhote-Alin Mts, USSR (Radkevich 1980). Also calc-silicate rocks of Stara Kamienica (Kowalski, Karwowski & *al.* 1978) and greisens of the Izera Highland (Karwowski 1977) bear similar mineral association, which confirms hydrothermal genesis of that mineralization.

(iii) Distinct role of tin in the sulfide paragenesis proves a close connection of cassiterite and later sulfides. The authors suppose that the source of hydrothermal solutions mineralizing the Kamienica Chain schists should be located in the Karkonosze granitoid massif and they include the studied deposits into the Variscan, Middle-European tin province.

*Institute of Analysis of Mineral Raw Materials  
of the Silesian University,  
ul. Mielczarskiego,  
41-200 Sosnowiec, Poland*

## REFERENCES

- BIRECKI T. 1959. The tin ore deposits at Przecznicza, Lower Silesia. *Zeszyty Naukowe AGH w Krakowie*, 22, (Geologia 3), 34—53. Kraków.
- CHILIŃSKA H. 1965. Perspectives in search for tin ore deposits in the light of metallogeny of the Sudetes. *Przepl. Geol.* 13 (1), 20—25. Warszawa.
- JASKÓLSKI S. 1963. Erwägungen über die Genese zinnführender Schiefer in Isergebirge (Niederschlesien). *Prace Geol. Kom. Nauk Geol. PAN*, 12, 33—50. Kraków.
- 1967. Tin deposits at Gierczyn. *Przepl. Geol.* 15 (5), 238, Warszawa.
- & MOCHNACKA K. 1968. Tin deposits at Gierczyn in Isera Mountains, Lower Silesia; an attempt of elucidating their origin. *Arch. Mineral.* 22 (1), 17—106. Warszawa.

- KARWOWSKI Ł. 1977. Geochemical conditions of greisenization in the Iżera Mountains foothills (Lower Silesia). *Arch. Mineral.*, **33** (2), 83—148. Warszawa.
- KOWALSKI W., KARWOWSKI Ł., SMIETAŃSKA I. & DO VAN PHI. 1978. Ore mineralization of the Stara Kamienica zone schist range in the Iżera Mountains. *Prace Naukowe Univ. Śląskiego. Geologia* **3**, 7—90. Katowice.
- KOZŁOWSKI A. & KARWOWSKI Ł. 1975. Genetic indications of tungsten-tin-molybdenum mineralization within the Karkonosze-Iżera block. *Kwart. Geol.*, **19** (1), 67—73. Warszawa.
- PUTZER H. 1940. Die Zinnführende Fahllagerstätten von Giehren am Isergebirge. *Zeitschr. d. Deutsch. Geol. Ges.*, **92** (3), Berlin.
- RADKEVICH E. A. [Editor] 1980. Geology, mineralogy and geochemistry of the Kavalerovo region, *Nauka*; Moskwa [in Russian].
- RAMDOHR P. 1975. Die Erzminerale und ihre Verwachsungen. *Akademie-Verlag*. Berlin.
- SACHS A. 1914. Die Bildung Schlesischer Erzlagerstätten. *Centralbl. f. Min.* Stuttgart.
- SALAĆIŃSKI R. 1965. Depositional and genetical problems of cassiterite-sulphide mineralization of the Iżera schists in the Czerniawa Zdrój area. *Biul. Geol.*, **5**, 85—91. Warszawa.
- SCHNEIDERHÖHN H. & RAMDOHR P. 1931. Lehrbuch der Erzmikroskopie. Berlin.
- STEHR H. 1933. Ein Beitrag zur Kenntniss d. Zinn-Kobalt Lagerstätte von Giehren-Querbach in Isergebirge. *Bergmännische Meldearbeit*. Clausthal.
- SZAŁAMACHA M. 1967. On tin mineralization in the eastern part of the Kamienica Belt in the Iżera Mountains. *Przeł. Geol.*, **15** (6), 281—284. Warszawa.
- 1970. Przejawy mineralizacji kasyterytowej w łupkach łyszczkowych Pasma Kamienieckiego na przykładzie kamieniołomu w Krobicy. *Kwart. Geol.*, **14** (3), 575—576. Warszawa.
- & SZAŁAMACHA J. 1974. Geological and petrographic characteristics of schists mineralized with cassiterite on the basis of materials from the quarry at Krobica. *Biul. Inst. Geol.*, **279**, 59—89. Warszawa.
- ZIMNOCH E. 1965. New data on the ore mineralization of deposits at Stara Góra. *Biul. Geol.*, **5**, 3—38. Warszawa.

---

Ł. KARWOWSKI i R. WŁODYKA

### STANNIN W ZŁOŻACH KASYTERYTOWO-SIARCZKOWYCH GÓR IZERSKICH

(Streszczenie)

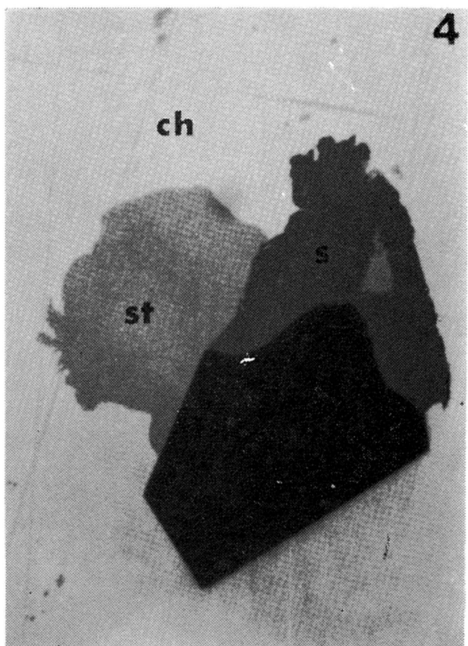
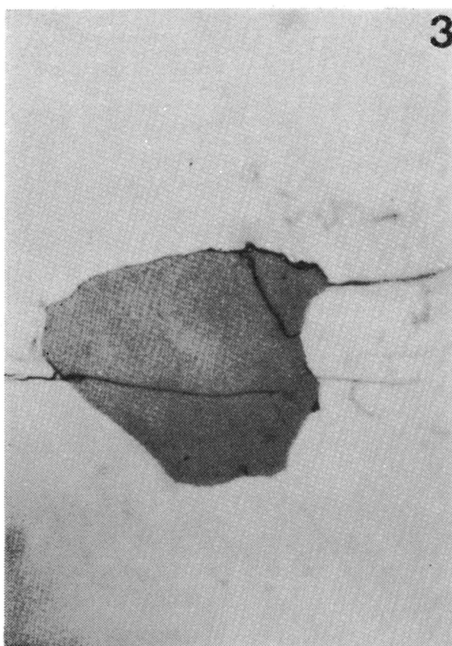
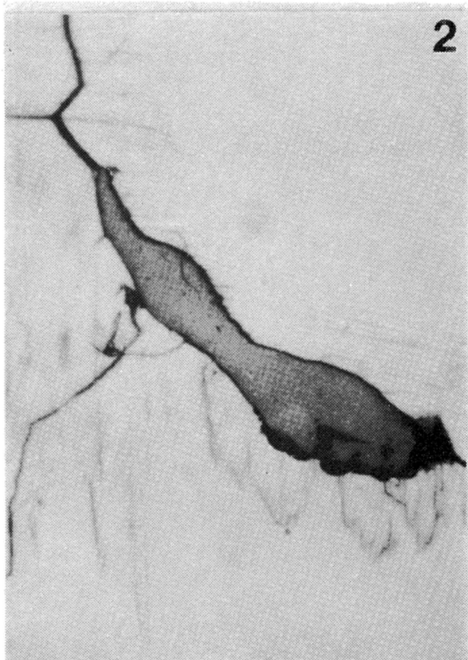
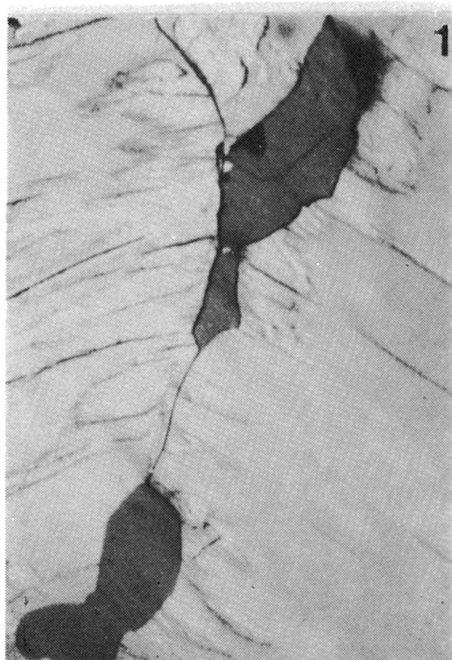
W złożach kasyterytowo-siarczkowych rejonu Gierczyna i Przeczniczy w Górach Izerskich (patrz fig. 1) stwierdzono występowanie stanninu, którego identyfikację potwierdzono badaniami w mikroanalizatorze rentgenowskim (patrz pl. 2, fig. 3—4 oraz pl. 3, fig. 1—2).

Stannin o składzie chemicznym odpowiadającym teoretycznemu (*patrz* tabela 1) występuje w ścisłej paragenezie z chalkopirytem, sfalerytem i pirotynem oraz wieloma minerałami siarczkowymi (*patrz* pl. 1—5). Stwierdzono także występowanie późnego posiarczkowego kasyterytu (*patrz* pl. 6).

Obecność stanninu oraz posiarczkowego kasyterytu w omawianych złożach świadczy o znacznej roli cyny w roztworach minerałotwórczych nie tylko w trakcie powstawania najwcześniejszej mineralizacji kasyterytowej, ale także w dalszym ciągu ewolucji roztworów powodujących wydzielanie się siarczków.

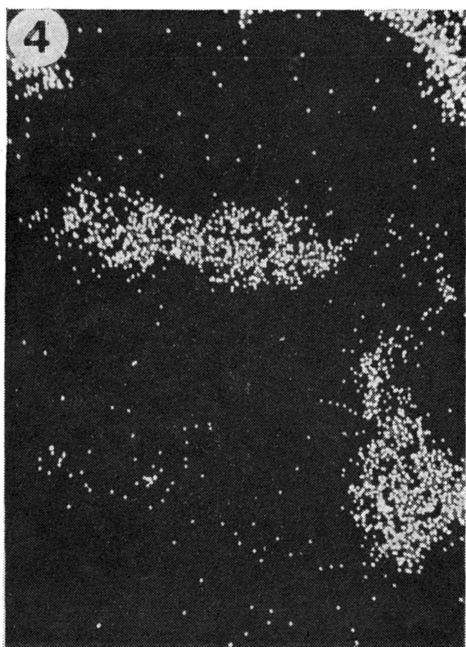
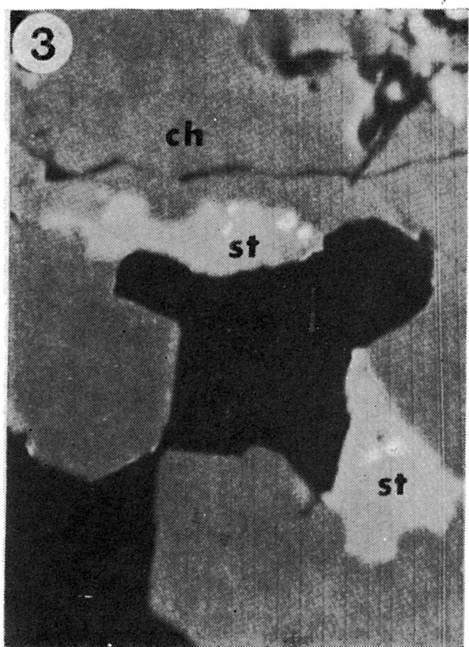
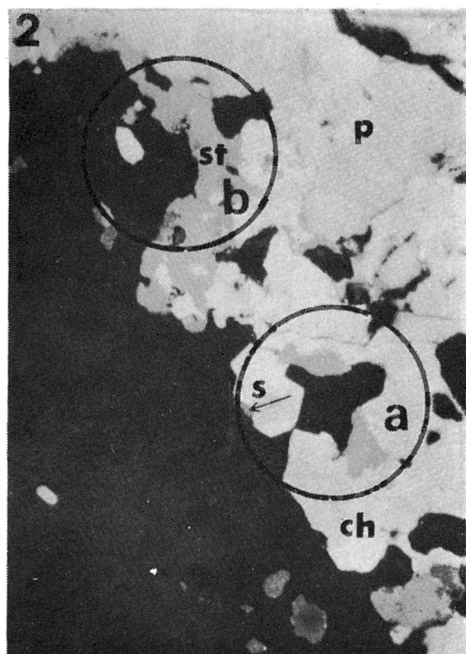
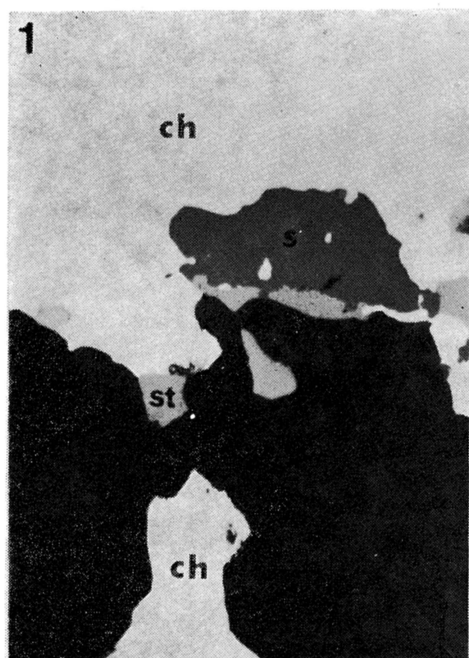
Przedstawione fakty wskazują na hydrotermalną genezę złóż kasyterytowo-siarczkowych Gór Izerskich i pozwalają wiązać je genetycznie z warycyjskim granitoidem Karkonoszy.

---

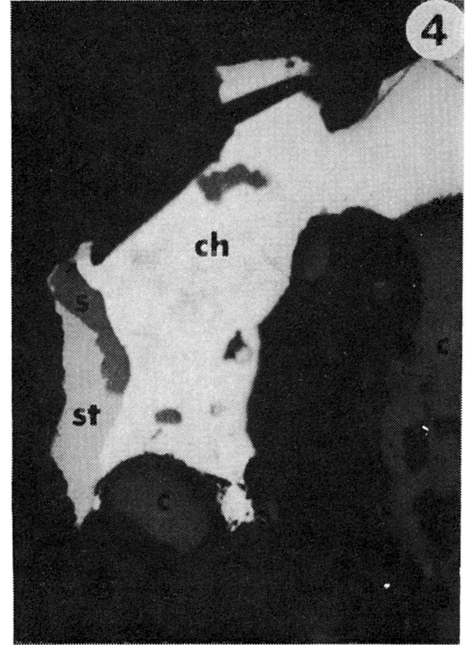
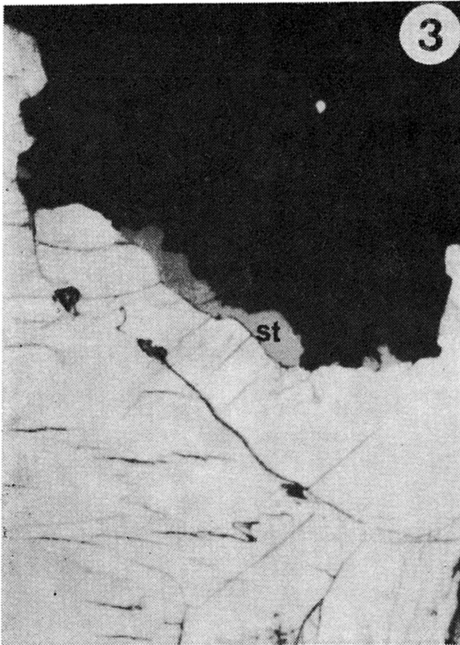
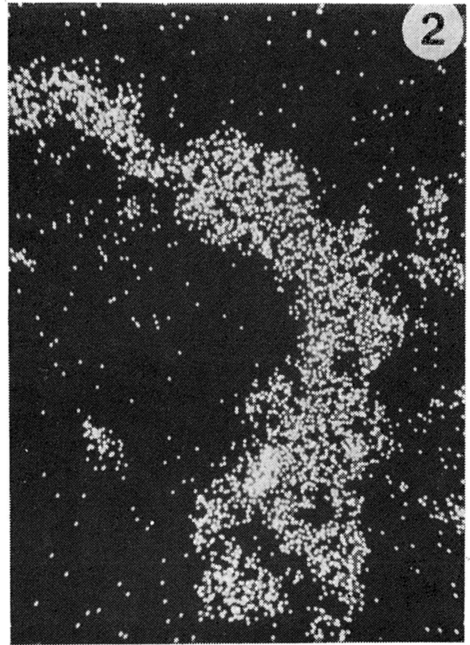
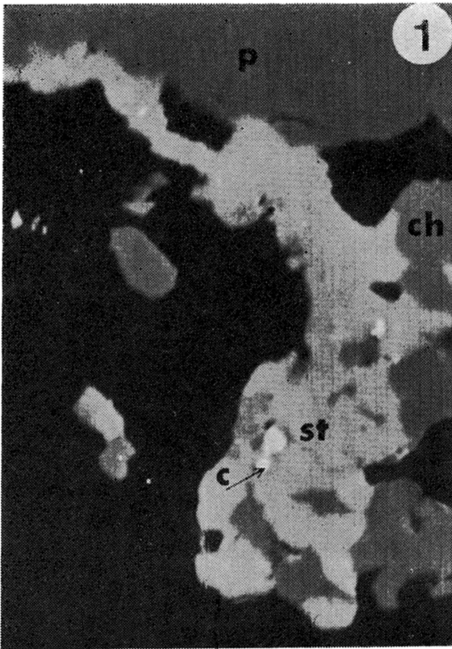


- 1 — Stannite (*gray*) in altered pyrrhotite; stannite distributed along fissures in pyrrhotite; one nicol, oil immersion;  $\times 3300$
- 2 — Stannite (*gray*) in fissure zones in pyrrhotite; one nicol, oil immersion;  $\times 3300$
- 3 — Stannite (*gray*) in pyrrhotite (*white*); fissures continue also in stannite; one nicol, oil immersion;  $\times 2300$
- 4 — Stannite (*st*; bireflectivity visible) and sphalerite (*s*) in chalcopyrite (*ch*); one nicol,  $\times 1300$

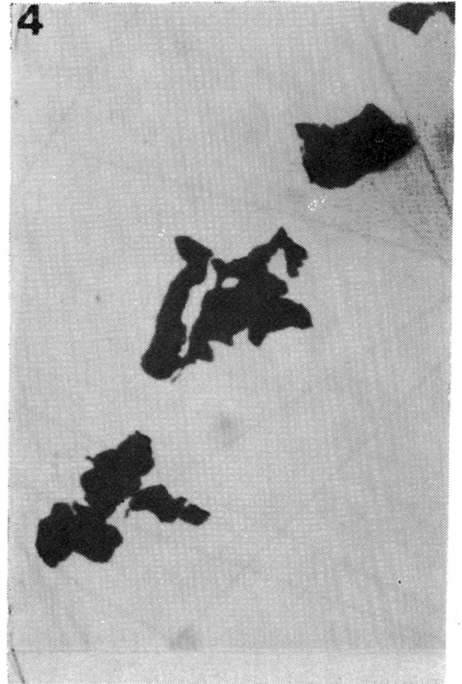
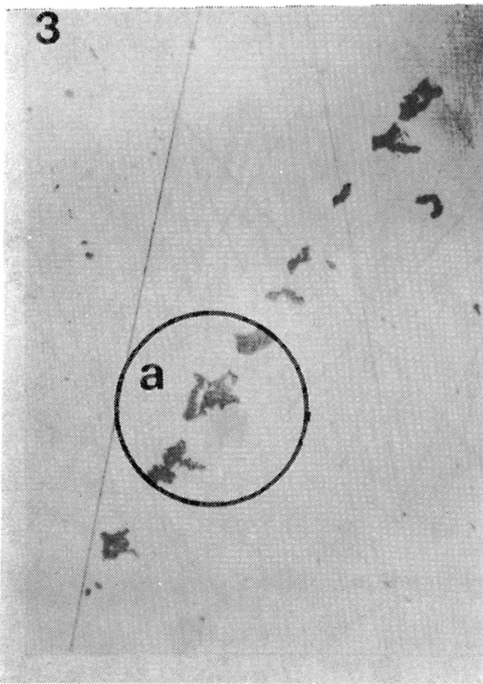
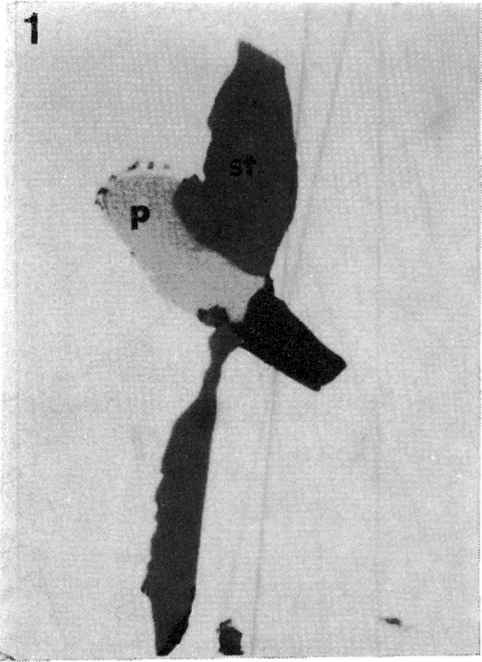




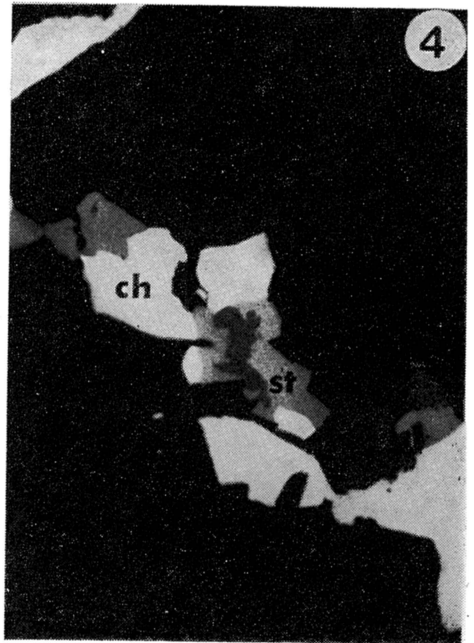
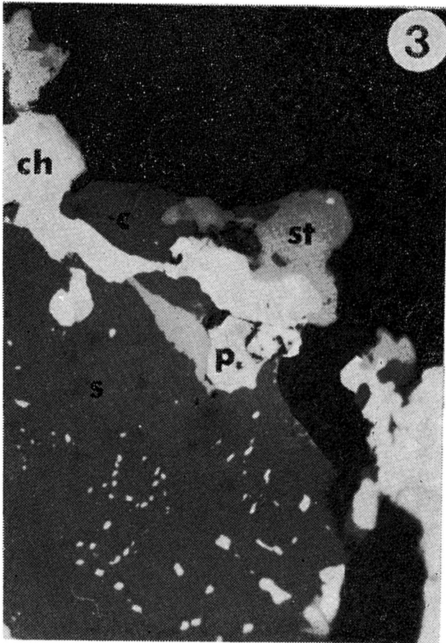
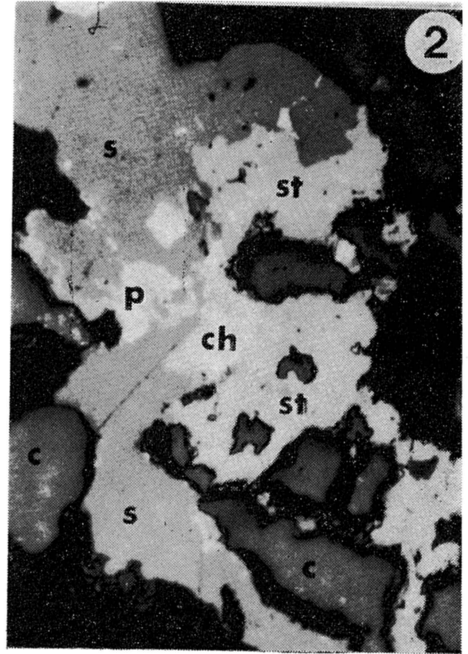
- 1 — Stannite (*st*) at the edges of sphalerite (*s*) and chalcopyrite (*ch*); black — quartz; one nicol,  $\times 750$
- 2 — Stannite (*st*) paragenetic with chalcopyrite (*ch*), pyrrhotite (*p*) and sphalerite (*s*); one nicol,  $\times 500$
- 3 — Close-up view of the detail *a* of Fig. 2: stannite (*st*) and chalcopyrite (*ch*); back-scattered electron image,  $\times 1550$
- 4 — Close-up view of the detail *a* of Fig. 2: tin distribution; Sn  $K\alpha$  radiation,  $\times 1550$



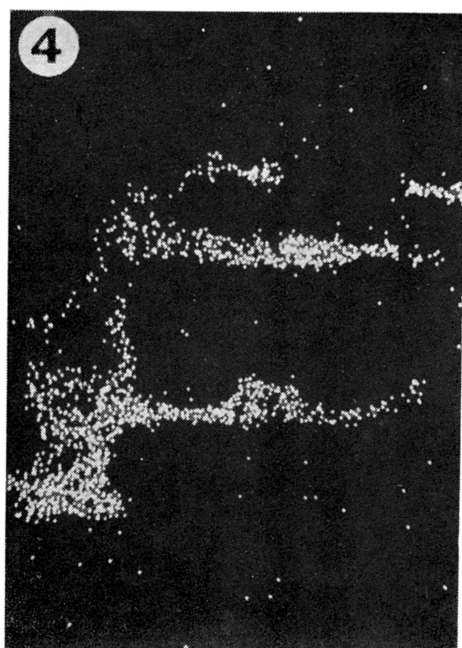
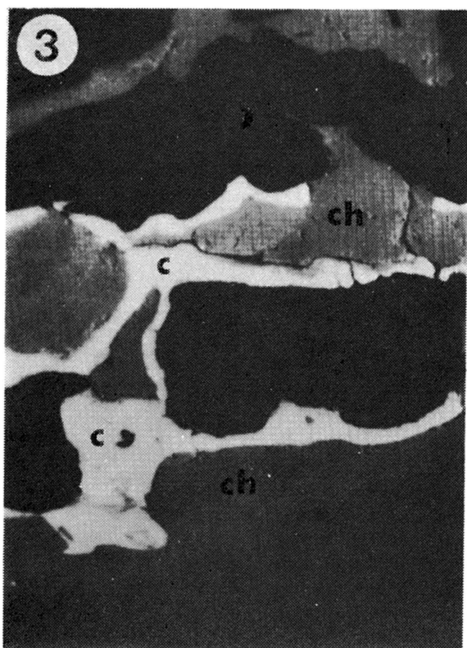
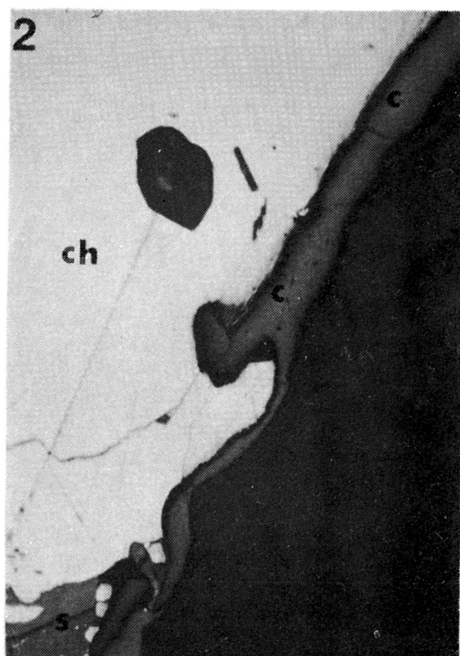
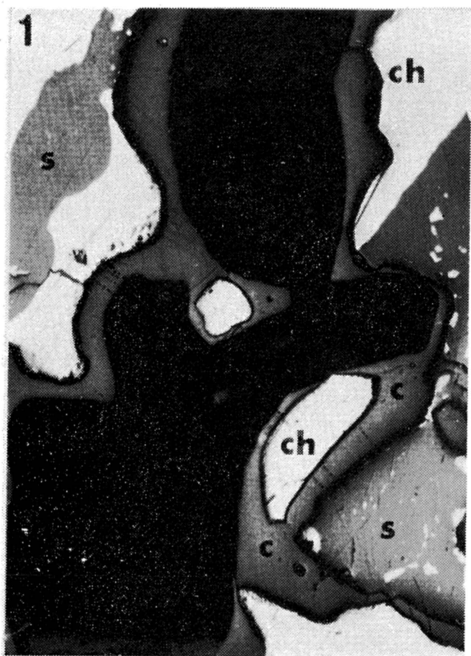
- 1 — Close-up view of the detail **b** of Pl. 2, Fig. 2: stannite (*st*), chalcopyrite (*ch*), pyrrhotite (*p*) and cassiterite (*c*); back-scattered electron image,  $\times 1330$
- 2 — Close-up view of the detail **b** of Pl. 2, Fig. 2: tin distribution; Sn  $K\alpha$  radiation,  $\times 1330$
- 3 — Stannite (*st*) at the boundary between pyrrhotite (*light*) and sphalerite (*black*) one nicol, oil immersion;  $\times 2250$
- 4 — Stannite (*st*) occurring with sphalerite (*s*), chalcopyrite (*ch*) and cassiterite (*c*); one nicol,  $\times 870$



- 1 — Intergrowth of stannite (*st*) with pyrrhotite (*p*) and sphalerite (*black*) occurring in chalcopyrite (*white*); one nicol, oil immersion;  $\times 2300$
- 2 — Parallel grains of stannite and sphalerite (*dark*) in chalcopyrite (*light*); one nicol, oil immersion;  $\times 700$
- 3 — Stannite inclusions (*st*) in chalcopyrite (*light*); one nicol;  $\times 700$
- 4 — Close-up view of the detail *a* of Fig. 3; one nicol, oil immersion;  $\times 2200$



- 1 — Occurrence of cassiterite (c), stannite (st), sphalerite (s) and chalcopyrite (ch); one nicol, oil immersion; X2200
- 2 — Stannite (st) bearing tiny chalcopyrite inclusions and occurring with sphalerite (s), pyrrhotite (p), chalcopyrite (ch) and cassiterite (c); one nicol, X1300
- 3 — Stannite (st) paragenetic with pyrrhotite (p), chalcopyrite (ch), cassiterite (c) and sphalerite (s) bearing chalcopyrite inclusions; one nicol, X700
- 4 — Occurrence of chalcopyrite (ch) and stannite (st), the latter bears sphalerite inclusion (dark gray); one nicol, X900



- 1 — Secondary cryptocrystalline cassiterite (c) surrounding chalcopyrite (ch) and sphalerite (s); one nicol,  $\times 320$
- 2 — Late cassiterite (c) at the edges of chalcopyrite (ch) and sphalerite (s) grains; one nicol,  $\times 400$
- 3 — Late cassiterite (c) surrounding chalcopyrite (ch); back-scattered electron image,  $\times 150$
- 4 — Same detail as in Fig. 3: tin distribution; Sn  $K\alpha$  radiation,  $\times 150$